

Selective ionization of Ba and Sr isotopes based on a two-photon interference effect

S. M. Park and G. J. Diebold

Department of Chemistry, Brown University, Providence, Rhode Island 02912

(Received 11 September 1989)

We show that the zero- and nonzero-nuclear-spin isotopes of Ba and Sr can be excited and ionized at different rates by sequential absorption of radiation from two pulsed laser beams. The selective excitation takes place in a $J=0 \leftarrow J=1 \leftarrow J=0$ energy-level scheme (where J is the electronic angular momentum), which, depending on the relative polarization of the laser beams, gives totally destructive interference in the absorption rate to the upper $J=0$ state of a zero-nuclear-spin atom, or a finite but time-dependent rate for population of the upper state for an atom with nonzero nuclear spin. A theoretical explanation of the effect shows the alignment of the nuclear spin as well as the population of the upper state to be time dependent. Isotope ratios were measured in Ba and Sr as a function of laser polarization and delay time, and compared with theory.

I. INTRODUCTION

In a simple $J=0 \leftarrow J=1 \leftarrow J=0$ energy-level scheme, the rate of nonresonant two-photon absorption (i.e., with the first photon off resonance with the $J=1 \leftarrow J=0$ transition) can become zero as a result of a quantum-mechanical interference effect.¹ When the electric vectors of two linearly polarized light beams are expressed as coherent superpositions of σ^+ and σ^- beams, two pathways with probability amplitudes \mathcal{P}_1 and \mathcal{P}_2 for population of the upper state exist, as shown in Fig. 1. When the electric vectors of the two light beams are parallel, the signs and amplitudes of \mathcal{P}_1 and \mathcal{P}_2 are identical, so the interference is constructive and the population rate of the upper state is finite; when the light-beam polarizations are orthogonal, a phase shift of π is introduced into the relative probability amplitude resulting in completely destructive interference with a population transfer rate to the final state of zero. This effect was recently observed in Sr where the degree of destructive interference was measured as a function of the angle between two linearly polarized laser beams by monitoring the population of the $7s \ ^1S$ state.²

On first inspection it is natural to conclude that orthogonally polarized laser beams could be used to populate selectively the upper 1S state of atoms with nonzero nuclear spin through nonresonant excitation of a $^1S \leftarrow ^1P \leftarrow ^1S$ sequence. That is, isotopes with no nuclear spin have energy-level schemes as shown in Fig. 1(a) and would not be excited in a nonresonant two-photon process owing to the interference effect. Isotopes with a nuclear spin I of 1, for instance, would be excited through pathways such as those shown in Fig. 1(a), but additional pathways, such as \mathcal{P}_3 shown in Fig. 1(b), where interference cannot take place, would always be present, so that irrespective of the light-beam polarizations, two-photon absorption would always occur.

Since absorption of a third photon from either of the two laser beams can ionize the excited atom, a clear discrimination against zero-nuclear-spin isotopes in the

ion current should be observed as the relative polarization of the two laser beams is rotated through angles from parallel to perpendicular. Surprisingly, experiments with ^{138}Ba and ^{137}Ba irradiated with 8-ns-long dye-laser pulses showed no statistically significant variation in the ratio of the ion currents from these two isotopes as the relative polarization of the radiation beams was varied—the presence of excitation paths such as \mathcal{P}_3 did not alter the isotope ratio.

In retrospect, the explanation for this behavior is elementary. The initiation of the first laser beam produces a “virtual state” that is a coherent superposition of coupled

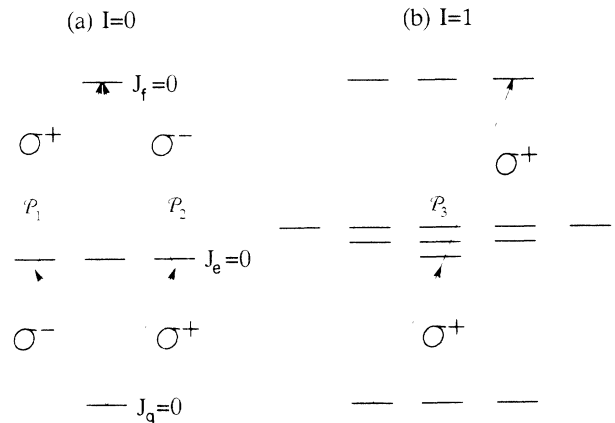


FIG. 1. (a) Energy-level diagram for a two-photon transition in a $J=0 \leftarrow J=1 \leftarrow J=0$ system. For nonresonant multiphoton absorption, the first light beam is detuned a small amount Δ in frequency from resonance with the first excited state. The arrows indicate absorption through the two paths: \mathcal{P}_1 represents the probability amplitude for absorption of a σ^- photon from the first beam, and a σ^+ photon from the second beam. (b) Energy-level diagram for an atom with nuclear spin $I=1$. Absorption of two σ^- photons is possible leading to population of the upper state irrespective of the relative polarization of the radiation beams.

angular momentum states. The time evolution of these states, governed by the magnitude of the hyperfine splittings, is sufficiently slow compared with the virtual-state lifetime that the flow of probability amplitude into states that can be excited by the second laser beam is negligible. Thus, the hyperfine interaction in the nonzero spin isotopes appears to be nonoperative or "frozen" on the time scale of the experiment as set by the magnitude of the detuning of the first laser beam from resonance.

As we show below, selective excitation of nonzero spin isotopes is possible using pulsed lasers provided the first laser is tuned to resonance with the first excited state and the state is allowed to evolve in time before the second laser is fired. Section II gives a theoretical explanation of the effect using the state multipole formalism. The calculations shown the monopole and quadrupole moments of the excited-state population to evolve as the delay time between the pulses is varied. Section III describes atomic-beam experiments with Ba and Sr atoms that show selective ionization of the odd atomic masses of these elements. Finally, Sec. IV shows how time evolution of coherently excited states can affect other multi-photon processes.

II. THEORY

A complete theory of the sequential two-photon excitation of an excited $J=0$ atomic state through a resonant $J=0 \leftarrow J=1 \leftarrow J=0$ sequence is given here using statistical tensors (state multipoles) to describe the angular momentum distribution in each state. Since the mathematics of this description gives little insight into the nature of the evolution of the states, a brief example of how the discrimination takes place is given for a nuclear spin $I = \frac{1}{2}$ atom.

Consider first an isotope with no nuclear spin. The first laser beam whose electric vector is parallel to the x axis excites the atom to a state $\psi_{J=1}(t)$ (referred to here as the excited state) given by

$$\psi_{J=1}(t) = \frac{1}{\sqrt{2}}(|1-1\rangle - |11\rangle)e^{-\Gamma t/2}, \quad (1)$$

where t is the time after excitation, Γ is the decay rate of the $J=1$ state, which is a coherent superposition of two $|JM_J\rangle$ states, where M_J is the magnetic quantum number, and where the z axis has been taken as the axis of quantization. The transition probability to the final state is proportional to $P(t)$ given by

$$P(t) = |\langle 00 | \epsilon_2 \cdot \mathbf{D} | \psi_{J=1}(t) \rangle|^2, \quad (2)$$

where ϵ_2 is the polarization vector of the second laser and \mathbf{D} is the electric dipole operator. The quantity $\epsilon_2 \cdot \mathbf{D}$ can be written in a spherical basis as

$$\epsilon_2 \cdot \mathbf{D} = \sum_q (-1)^q \epsilon_q^{\lambda_2} D_{-q} \quad (3)$$

according to the usual definitions³ of these quantities, so that $P(t)$ becomes

$$P(t) = \frac{1}{2} |\langle 00 | \epsilon_{+1}^{\lambda_2} D_{-1} | 11 \rangle - \langle 00 | \epsilon_{-1}^{\lambda_2} D_{+1} | 1-1 \rangle|^2 e^{-\Gamma t}, \quad (4)$$

which for ϵ_2 parallel to the y axis ($\epsilon_{\pm} = -i/\sqrt{2}$) can easily be shown to equal zero.

Consider an atom with nuclear spin $I = \frac{1}{2}$. Excitation of the $|00\rangle |I = \frac{1}{2}, M_I = \frac{1}{2}\rangle$ state (in a basis set that is a product of electronic and nuclear wave functions, where M_I is the magnetic quantum number for the nuclear spin) by the same x -polarized light beam (where the laser bandwidth is large compared with the hyperfine splitting), gives the $J=1$ state in an uncoupled basis as

$$\psi(0)_{J=1, \text{uncoupled}} = \frac{1}{\sqrt{2}}(|1-1\rangle - |11\rangle) | \frac{1}{2} \frac{1}{2} \rangle. \quad (5)$$

This state can be expressed in a coupled basis set $|FM_F\rangle$ where its time evolution in the Schrödinger picture is given as

$$\begin{aligned} \psi(t)_{J=1, \text{coupled}} &= \sum_{F, M_F} |FM_F\rangle \langle FM_F | \psi(0)_{J=1, \text{coupled}} \rangle e^{-(iE_F t/\hbar)} e^{-(\Gamma t/2)} \\ &= \left[\frac{1}{\sqrt{6}} \left| \frac{3}{2} - \frac{1}{2} \right\rangle e^{-i\omega_{3/2} t} - \frac{1}{\sqrt{3}} \left| \frac{1}{2} - \frac{1}{2} \right\rangle e^{-i\omega_{1/2} t} - \frac{1}{\sqrt{3}} \left| \frac{3}{2} \frac{3}{2} \right\rangle e^{-i\omega_{1/2} t} \right] e^{-(\Gamma t/2)}, \end{aligned} \quad (6)$$

where $\omega_{3/2}$ and $\omega_{1/2}$ are the energies of the $F = \frac{3}{2}$ and $\frac{1}{2}$ hyperfine state divided by \hbar , respectively. This wave function can then be rewritten in the uncoupled basis as

$$\begin{aligned} \psi(t)_{J=1, \text{uncoupled}} &= \left[\frac{1}{\sqrt{18}} e^{-i\omega_{3/2} t} + \frac{\sqrt{2}}{3} e^{-i\omega_{1/2} t} \right] |1-1\rangle | \frac{1}{2} \frac{1}{2} \rangle e^{-(\Gamma t/2)} \\ &\quad + \frac{1}{3} (e^{-i\omega_{3/2} t} - e^{-i\omega_{1/2} t}) |10\rangle | \frac{1}{2} - \frac{1}{2} \rangle e^{-(\Gamma t/2)} - \frac{1}{\sqrt{2}} e^{-i\omega_{3/2} t} |11\rangle | \frac{1}{2} \frac{1}{2} \rangle e^{-(\Gamma t/2)}. \end{aligned} \quad (7)$$

which together with Eq. (2) gives $P(t)$. The absorption rate in the weak-field limit becomes

$$P(t) = \frac{4}{9} e^{-\Gamma t} \sin^2 \left[\frac{\Delta \omega t}{2} \right], \quad (8)$$

where $\Delta \omega = \omega_{3/2} - \omega_{1/2}$. Calculation of the excitation rate from the $|00\rangle|\frac{1}{2}-\frac{1}{2}\rangle$ sublevel of the ground state gives an identical expression that is added to Eq. (8) to give the total population rate of the final state. It is thus evident that a nonzero probability for excitation of the final state can be obtained by suitable delay of the second laser relative to the first and that selective excitation of spin- $\frac{1}{2}$ isotopes possible. A transition probability dependent on time delay as is shown below is a general property of systems with finite nuclear spin. In addition, multipole moments of the nuclear angular momentum of the final state with rank 2 or less can be created by absorption of two photons.

Consider the description of the above problem⁴ in terms of density matrices⁵ of the ground state ρ^g , excited state ρ^e and final state ρ^f . The ground state is described by a single, rank zero term.⁶ The time evolution of the upper states is described by the rate equations for the density matrices that include the effects of radiative de-

cay and hyperfine coupling.⁷ Immediately after firing of the first laser, the excited-state density matrix can be written as

$$\begin{aligned} \rho^e = \frac{1}{3} \sum_{p,p'} (-1)^{p+J_e+J_g} e_{-p}^{\lambda_1} e_{-p'}^{\lambda_1^*} \frac{1}{\sqrt{(2J_g+1)(2I+1)}} \\ \times |\langle J_e \| D \| J_g \rangle|^2 \\ \times T_{1-p}(J_e J_g) T_{00}(J_g J_g) T_{1p'}(J_g J_e) T_{00}(II), \end{aligned} \quad (9)$$

where I is the nuclear-spin quantum number, J is the total electronic-angular-momentum quantum number of the state indicated by the subscript, T_{KQ} is a tensor operator of rank K (see Refs. 8–10), $e_p^{\lambda_1}$ is a component of the polarization vector of the exciting radiation expressed in a spherical basis (p takes on values of ± 1 and 0) for the first laser beam and $\langle J_e \| D \| J_g \rangle$ is a reduced matrix element. Next, the tensor operators are recoupled so that ρ^e is expressed in a coupled basis (where $F = I + J$); the hyperfine operator is then diagonal and the time dependence of ρ^e can be calculated. This gives ρ^e as a function of the time t after firing of the first laser as

$$\begin{aligned} \rho^e(t) = \frac{1}{3} \sum_{k,q,p,p',F_e,F_e'} (-1)^{p+F_e'+k+I} e_{-p}^{\lambda_1} e_{-p'}^{\lambda_1^*} |\langle 1 \| D \| 0 \rangle|^2 \frac{\sqrt{(2F_e+1)(2F_e'+1)}}{2I+1} \\ \times \langle 1-p; 1p' | kq \rangle \left\{ \begin{matrix} 1 & 1 & k \\ F_e & F_e' & I \end{matrix} \right\} T_{kq}(F_e F_e') e^{(i\omega_{F_e F_e'} - \Gamma)t}, \end{aligned} \quad (10)$$

where $\langle 1-p; 1p' | kq \rangle$ is a Clebsch-Gordan coefficient, the quantity in braces is a $6-j$ symbol, and $\omega_{F_e F_e'}$ is an angular frequency corresponding to the energy difference between the states F_e and F_e' . To determine the effect of the second laser beam, Eq. (10) is first expressed in the uncoupled basis, operated on by the electric dipole operator for the second laser beam, and integrated to give the density matrix ρ^f , which is expressed as a function of t , the time between firing of the two lasers. The density matrix of the final state is

$$\begin{aligned} \rho^f(t) = \sum_{p,p',p'',p''',F_e,F_e',k,k',q,q',K,Q,Q'} \frac{\sqrt{3}}{27} \frac{(-1)^{p+p''+F_e'+k-k'+Q'+I}}{2I+1} (2F_e+1)(2F_e'+1) \\ \times (2K+1)(2k+1)\sqrt{(2k'+1)} |\langle 1 \| D_{eg} \| 0 \rangle|^2 |\langle 0 \| D_{fe} \| 1 \rangle|^2 e_{-p}^{\lambda_1} e_{-p'}^{\lambda_1^*} e_{-p''}^{\lambda_2} e_{-p'''}^{\lambda_2^*} \\ \times \begin{bmatrix} 1 & 1 & k \\ -p & p' & -q \end{bmatrix} \begin{bmatrix} K & k' & k \\ Q & q' & -q \end{bmatrix} \begin{bmatrix} K & 1 & 1 \\ Q & p''' & -Q' \end{bmatrix} \begin{bmatrix} 1 & 1 & 0 \\ -p'' & Q' & 0 \end{bmatrix} \\ \times \begin{bmatrix} 1 & 1 & k \\ F_e & F_e' & I \end{bmatrix} \begin{bmatrix} 1 & 1 & K \\ I & I & k' \\ F_e & F_e' & k \end{bmatrix} e^{(i\omega_{F_e F_e'} - \Gamma)t} T_{00}^J(00) T_{k'q'}^I(II). \end{aligned} \quad (11)$$

The summation is over values of the polarization indices that describe the light beams the hyperfine states F_e , k and K which range from 0 to 2, k' which ranges from 0 to $2I$, and the magnetic quantum numbers Q , Q' , and q' which take on values determined by the total angular-

momentum quantum number.^{8–10}

It can be seen that Eq. (11) describes a sum over tensor operators $T_{k'q'}^I(II)$ of the form

$$\rho^f(t) = \sum_{k'q'} \langle T_{k'q'}^\dagger(II) \rangle T_{k'q'}(II). \quad (12)$$

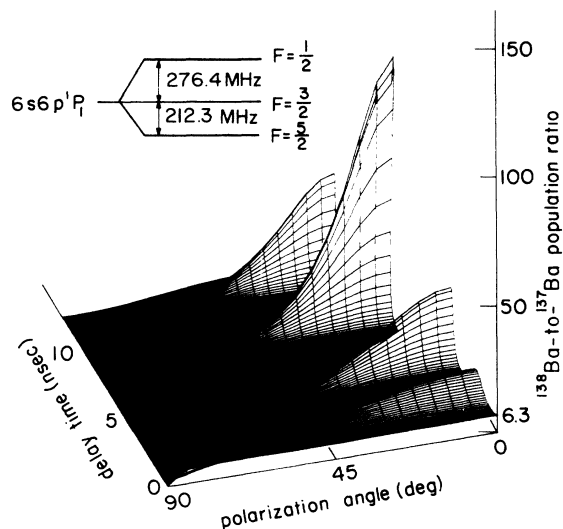


FIG. 2. Ratio of the ^{138}Ba to ^{137}Ba populations in the final state calculated from Eq. (11) as a function of the delay time between the two lasers and their relative (linear) polarization. The lifetime of the $J=1$ excited state is taken as 8.37 ns. The hyperfine energy level scheme (Ref. 12) for the $J=1$ excited state of ^{137}Ba is shown in the inset.

The time-dependent state multipoles $\langle T_{k'q'}^{\dagger}(II) \rangle$ are found from Eq. (11) as coefficients of the tensor operators $T_{k'q'}(II)$. The rank of the state multipoles of the nuclear angular momentum in the final state according to Eq. (11) ranges from 0 to $2I$. From Eq. (11) the monopole moments (populations) of the final state can be calculated for ^{138}Ba and ^{137}Ba as a function of delay time between the two lasers and as a function of the angle between the laser polarization vectors. Under the assumption that the ion-

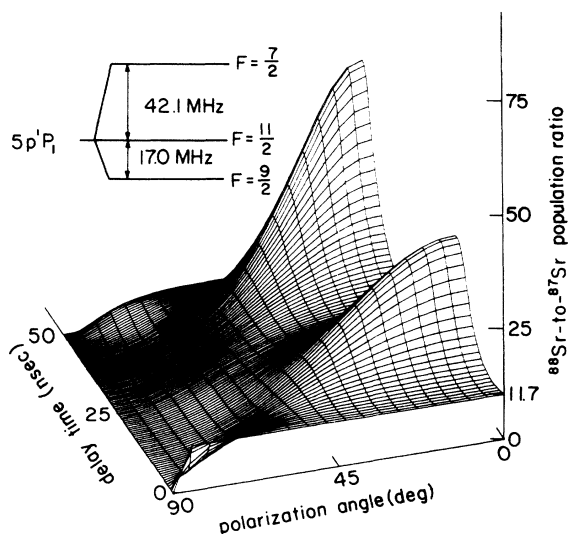


FIG. 3. Ratio of ^{88}Sr to ^{87}Sr populations in the final state as a function of laser delay time and relative polarization. The excited state lifetime is taken as 4.77 ns. The hyperfine energy level scheme (Ref. 12) of the ^{87}Sr excited state is shown in the inset.

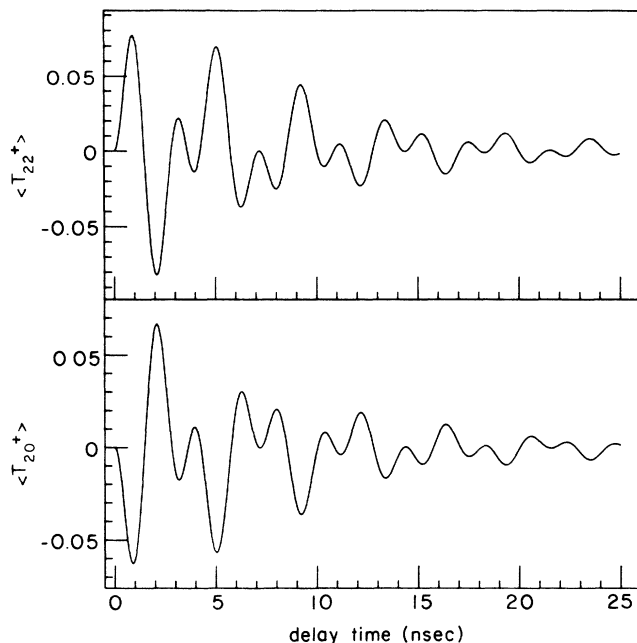


FIG. 4. Production of a nuclear quadrupole moment in the final $J=0$ state of ^{137}Ba as a function of delay time for two laser beams polarized along the x axis. The upper trace is $\langle T_{22}^{\dagger}(\frac{3}{2}, \frac{3}{2}) \rangle$ and the lower trace is $\langle T_{20}^{\dagger}(\frac{3}{2}, \frac{3}{2}) \rangle$ in dimensionless units.

ization signal is proportional to the final state population,¹¹ a time-dependent isotope ratio can be calculated. Such plots are given in Figs. 2 and 3 for two isotopes of Ba and Sr. The insets in each figure show the hyperfine structure of the intermediate excited state for ^{137}Ba and ^{87}Sr .¹² The variation in intensity of the isotope ratios follows as a consequence of the existence of three hyperfine states that give rise to several frequency components in the final state population that add in phase or out of phase as a function of time.

The production of a nuclear quadrupole moment in a final state can be seen as a function of the delay time between the two lasers in Figs. 4(a) and 4(b) where the $q'=0$ and 2 components of the second-rank tensor $T_{2q}(II)$ are plotted for ^{137}Ba (with $I=\frac{3}{2}$).

III. EXPERIMENTAL RESULTS

Experimental measurements of isotope ratios in atomic beams of Ba and Sr were made by averaging the ion current from a quadrupole mass spectrometer (Extrel, Inc. Model No. 4-162-8-125) in a boxcar averager (EGG-PAR, Inc., Model No. 162/64). The laser beams were directed (unfocussed) into the ionizer region of the mass spectrometer, the resulting ions were then focussed and accelerated into the mass filter. The dye lasers were pumped by harmonics of a Nd:YAG laser that operated at 10 Hz (YAG denotes yttrium aluminum garnet). As is shown in Fig. 5, an optical delay was inserted into the path of the second dye laser. Experiments were done in a differentially pumped high-vacuum chamber operated at a pressure of less than 1×10^{-8} atm (5×10^{-6} torr).

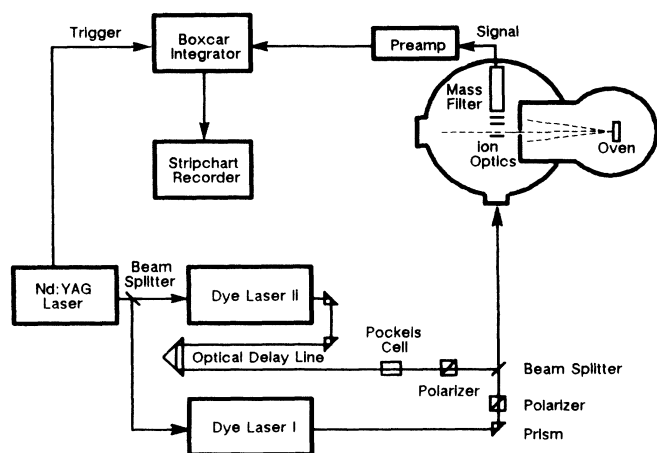


FIG. 5. Schematic diagram of the experimental apparatus. The Nd:YAG laser produced pulses on the order of 10-ns long.

Atomic beams with divergences of 2 mrad were produced by vaporizing Ba and Sr metal (with naturally occurring isotope ratios) in an electrically heated oven. The linewidth of the first dye laser was 0.012 nm (10-GHz full width at half maximum) as determined in a separate laser-induced fluorescence experiment. As a consequence of the small ion signals found in these experiments, the mass filter could not be operated to completely resolve the various masses. Ion current ratios were therefore computed from peak heights in the spectrum and thus do not represent exactly the isotope ratios in the elements.

A Pockels cell was used to rotate the polarization direction of the second dye laser. Polarizers were placed in the paths of both laser beams to improve the degree of polarization of each beam and to provide a means of accurately measuring the polarization direction of the beams. The laser beams were combined in a dichroic beam splitter. The variation in intensity of the second dye laser beam was measured to be less than 2% as its polarization angle was varied from 0 to 90°. Clearly, the degree of polarization of both beams determines the extent to which a convolution of the results of the previous section over orthogonal polarizations and a subsequent degradation of the polarization effects takes place. In addition, maintaining a constancy of overlap in space between the beams where they intersect the atomic beam is also important in an experiment.

The polarizers used for both beams were specified by the manufacturers to have extinction ratios of better than 10^4 , although the actual degree of polarization of the light beams after passing through the vacuum chamber windows was not measured. However, since the degree of polarization of the laser beams could not be increased to an arbitrarily high value, the procedure here has been to accept what could be realized with standard optical components and to use the resulting ion signals from the imperfect polarization as a reference for calculation of ratios. This procedure permitted the qualitative features of the effect to be observed.

An initial nonresonant experiment was done with the first dye laser tuned to 553.1 nm, which is 390 GHz off resonance with the $6s6p\ ^1P_1$ state of Ba. This detuning is approximately three orders of magnitude greater than the hyperfine splittings within the 1P_1 state. The second laser was tuned to 613.3 nm to excite the $6s8s\ ^1S_0$ state through a two-photon nonresonant process. As shown in Fig. 6, the ratio of the ^{138}Ba to ^{137}Ba ion signal showed no significant variation as the angle between the polarization vectors of the two lasers was varied from parallel to perpendicular.

In a resonant excitation when a time delay is introduced between the two laser beams, according to Sec. II above, it is possible to ionize ^{137}Ba selectively (relative to ^{138}Ba). With the first and second dye lasers tuned to 553.5 and 612.9 nm respectively to excite resonantly the sequence $6s8s\ ^1S_0 \leftarrow 6s6p\ ^1P_1 \leftarrow 6s^2\ ^1S_0$ and with a delay of 12 ns between the two laser beams, the Ba mass spectrum was recorded as a function of angle between the polarization vectors of the two lasers. Separate experiments done over a range of about three orders of magnitude in the intensities of both laser beams indicated that no saturation effects were present in the ion signal. The data as shown in Fig. 6 show a clearly observable change in the ^{138}Ba to

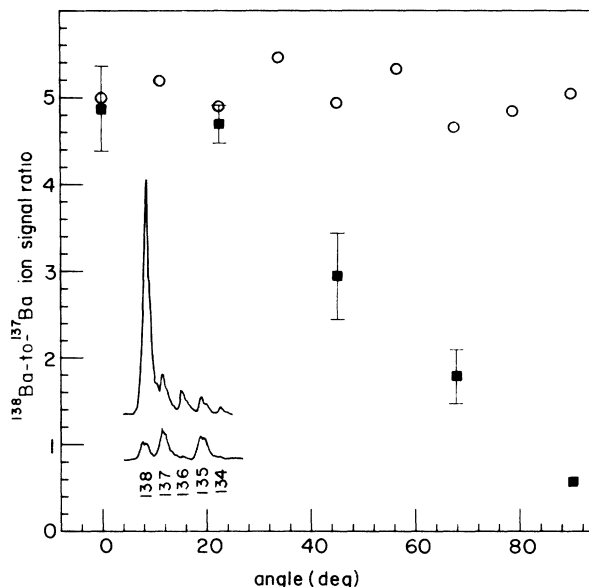


FIG. 6. ^{138}Ba to ^{137}Ba ion current ratio in the mass spectrometer vs relative polarization of the two dye laser beams. Open circles are data taken with the first laser beam 390 GHz below resonance and with no delay between the lasers. The laser intensities were 2.8 and 260 kW/cm² for the first and second laser, respectively. Squares are data taken with the lasers on resonance with a 12-ns delay between the two lasers. The first and second dye lasers delivered 35 W/cm² and 65 kW/cm², respectively. The error bars represent the experimental error (two standard deviations) for three different data sets. The inset shows representative mass spectra taken with parallel (upper spectrum) and perpendicular (lower spectrum) polarizations taken with a 12-ns delay.

^{137}Ba ion current ratio in the mass filter as the relative polarization of the two dye laser beams is rotated from parallel to perpendicular. The distinction between the resonant and nonresonant experiments is evident: given the comparatively short pulse widths of the lasers used here, the time evolution of the excited-state probability amplitudes can be used for selective excitation only when the first laser is on resonance and the excited-state lifetime is governed by the comparatively slow process of radiative decay.

Observation of the degree of constructive (or destructive) interference as a function of time in Ba is made difficult by the long pulsewidth of the laser relative to the hyperfine precession period. Although experiments were done to measure isotope ratios as a function of time with a fixed, perpendicular polarization, the data showed no variation over a 0- to 20-ns delay range. Given the approximately 8-ns-long laser pulsewidth, this result is expected based on the rapid variations seen in the isotope ratio plot for the final-state population shown in Fig. 2. The splittings in ^{87}Sr are significantly smaller than those in ^{137}Ba , and permit the effect of the time delay between the laser pulses to be seen without significant reduction in the modulation depth in the isotope ratio as a result of the finite laser pulsewidth. Data were taken with the laser polarization vectors perpendicular as the delay time was varied. The data for ^{87}Sr shown in Fig. 7 are normal-

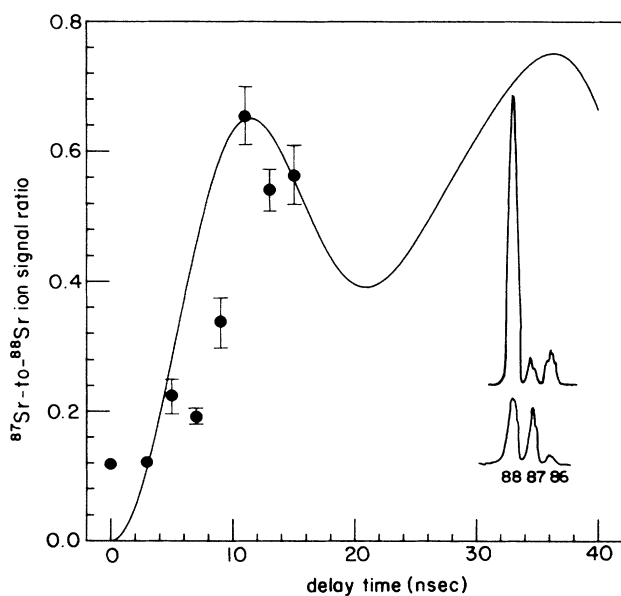


FIG. 7. Ratio of ion signals from ^{87}Sr to that from ^{88}Sr as a function of delay time between laser pulses using orthogonal laser polarizations. The solid curve is calculated from Eq. (11). The dye-laser intensities were 95 W/cm^2 and 86 kW/cm^2 for the first and second lasers, respectively. The ^{88}Sr signal is nonzero owing to imperfect polarization of the light beams and is used only to normalize the data. Note that the atomic beam density was increased to generate adequate signals in the experiments with the longest time delays. The inset shows representative mass spectra taken with parallel laser polarizations and no time delay between the two lasers (upper spectrum), and with perpendicular laser polarizations and an 11-ns delay between the two lasers (lower spectrum).

ized to the ^{88}Sr ion signal recorded at each time delay. The ^{88}Sr signal for perpendicularly polarized beams should, of course, be zero for any time delay; the observed signal is the result of imperfect polarization of the light beams. The advantage of calculating an isotope ratio is that the effect of the finite lifetime of the 1P state is eliminated in the resulting plot. The time evolution of the ^{87}Sr ion signal in Fig. 7 is in reasonably good agreement with Eq. (11). Some loss in modulation depth is, of course, expected in the experimental data since the laser pulses had a finite time duration.

An additional experiment was done where the ^{88}Sr to ^{87}Sr ion current was measured as a function of relative laser polarization at a fixed time delay. For an 11-ns-delay a pronounced falloff in this ratio was found as the polarizations were varied from parallel to perpendicular similar to that for Ba, as shown in Fig. 3. For zero time delay between the laser pulses only a small variation in the ion ratio was observed as the polarization angle was varied, the amount of decrease being consistent with the pulsewidth of the laser beams.

IV. CONCLUSION

It is clear from the experimental results given here that it is possible to excite selectively and ionize nonzero-spin atoms relative to zero-spin atoms based on destructive interference in the excitation pathways in a $J_f=0 \leftarrow J_e=1 \leftarrow J_g=0$ two-photon resonant sequence. A necessary condition for discrimination between zero and nonzero nuclear spin atoms is that a sufficient time delay be introduced before the second laser pulse interacts with the sample so that the probability amplitudes in the excited state depart from their values immediately after absorption of the first laser pulse. This conclusion has also been reached by the workers^{13,14} considering somewhat different excitation pathways. It is also evident that under the conditions of the experiments described here no such selective excitation of isotopes takes place in nonresonant two-photon absorption. This conclusion is not expected to hold universally under all experimental conditions; in fact, it can be argued that for sufficiently small detuning of the first laser from resonance, or for long laser pulsewidths compared with the hyperfine precession period, the opposite result might obtain.

In addition to the straightforward effects described here in the excitation of atoms, a general principle about the observation of small splittings in double resonance studies follows, namely, when short pulses are used to probe any atomic or molecular splitting, the presence of the splitting will be manifest in the two-photon spectrum only when the precession period of the interaction giving rise to the splitting is short compared with laser pulsewidth, and when the second probe is initiated after an appropriate delay time to allow sufficient development of the coherent superposition of states created by the first pulse.

ACKNOWLEDGMENTS

The authors are grateful for support of the work by the U.S. Department of Energy, Office of Basic Energy Sciences under Grant No. ER13235. The equipment grant by the U.S. Department of Defense is also acknowledged.

- ¹G. J. Diebold, *Phys. Rev. A* **32**, 2739 (1985).
- ²R. B. Stewart, G. J. Diebold, *Phys. Rev. A* **34**, 2547 (1986).
- ³C. Corney, *Atomic and Laser Spectroscopy* (Oxford University Press, New York, 1977).
- ⁴For further details of this calculation and the experiments described here see S. M. Park, Ph. D. thesis, Brown University, 1990.
- ⁵W. Happer, *Rev. Mod. Phys.* **44**, 169 (1972).
- ⁶K. Blum, *Density Matrix Theory and Applications* (Plenum, New York, 1981).
- ⁷G. Nienhuis, E. H. A. Granneman, and M. J. van der Wiel, *J. Phys. B* **11**, 1203 (1977).
- ⁸D. M. Brink and G. R. Satchler, *Angular Momentum* (Clarendon, London, 1968).
- ⁹A. R. Edmonds, *Angular Momentum in Quantum Mechanics* (Princeton University Press, Princeton, New Jersey, 1974).
- ¹⁰B. L. Silver, *Irreducible Tensor Methods—An Introduction for Chemists* (Academic, New York, 1976).
- ¹¹There are circumstances where the isotope ratios in the ion signal does not correspond to that in the neutral sample. See W. M. Fairbank, Jr., M. T. Spaar, J. E. Parks, and J. M. R. Hutchinson, *Inst. Phys. Conf. Ser.* **94**, 293 (1988).
- ¹²H. J. Kluge and H. Santer, *Z. Phys.* **270**, 295 (1974).
- ¹³L. C. Balling and J. J. Wright, *Appl. Phys. Lett.* **29**, 411 (1976).
- ¹⁴Ya. B. Zeldovich and I. I. Sobelman, *Pis'ma Zh. Eksp. Teor. Fiz.* **21**, 368 (1975) [*JETP Lett.* **21**, 168 (1975)].